



# Temperature-dependent multiphase chemical kinetics can explain uniform atmospheric nanoparticle growth rates

Zhiqiang Zhang<sup>1</sup>, Hyun Gu Kang<sup>1</sup>, Ulrich Pöschl<sup>1</sup>, and Thomas Berkemeier<sup>1</sup>

<sup>1</sup>Multiphase Chemistry Department, Max Planck Institute for Chemistry, Hahn-Meitner-Weg 1, 55128 Mainz, Germany

**Correspondence:** Thomas Berkemeier (t.berkemeier@mpic.de)

## Abstract

Aerosols have a profound influence on climate and human health, but new particle formation in the atmosphere has remained a scientific conundrum. In particular, the growth rates of atmospheric nanoparticles are often smaller and less dependent on condensable vapor concentration than expected. Here, we take a new integrative approach to analyze observational data from field measurements and chamber experiments, which were previously unexplained and appeared inconsistent with theory and model predictions. We show that the observed growth rates can be predicted when the temperature dependence and multiphase kinetics of gas-particle partitioning are resolved. Slow surface-to-bulk transport limits the rates of vapor uptake by semi-solid particles with low diffusivity, whereas shifts in the volatility distribution following the Clausius-Clapeyron equation enhance growth rates at low temperature and concentration levels. These antagonistic effects lead to an effective buffering of the organic vapor concentration dependence of nanoparticle growth in secondary organic aerosols. Our study reveals how counteracting temperature dependencies of organic vapor oxidation, volatility and multiphase kinetics lead to a convergence of growth rates around a few nanometers per hour under widely differing atmospheric conditions.

## 1 Introduction

Atmospheric aerosols consisting of airborne particles in the nanometer to micrometer size range have a strong influence on air quality, public health, and climate (IPCC, 2023; WHO, 2023). Large fractions of airborne fine particulate matter consist of secondary organic aerosols (SOA) formed by gas-to-particle conversion of organic precursor molecules in the atmosphere (Jimenez et al., 2009; Riipinen et al., 2011; Shrivastava et al., 2017). Over the past decades, numerous studies have investigated atmospheric new particle formation and growth (Kulmala et al., 2004, 2014; Stolzenburg et al., 2023). The rates of nanoparticle growth, however, have remained enigmatic and constitute a major gap in the scientific understanding and assessment of atmospheric aerosols and their effects on health and climate (Bianchi et al., 2016; Gordon et al., 2017; Kulmala et al., 2022). In particular, the growth rates of SOA nanoparticles observed in field measurements and laboratory experiments could not be explained by the traditional kinetic models applied in earlier studies (Stolzenburg et al., 2018; Yli-Juuti et al., 2020; Stolzenburg et al., 2025).



Under atmospheric conditions, organic aerosol particles are expected to exist in highly viscous or semi-solid phase states and may even exhibit an amorphous solid (glassy) state at low temperatures and humidities (Zobrist et al., 2008; Mikhailov et al., 2009; Virtanen et al., 2010; Koop et al., 2011; Renbaum-Wolff et al., 2013; Shiraiwa et al., 2017; Reid et al., 2018). Accordingly, the molecular diffusivity in SOA particles can vary over a wide range from more than  $10^{-10}$   $\text{cm}^2 \text{s}^{-1}$  (liquid) to less than  $10^{-21}$   $\text{cm}^2 \text{s}^{-1}$  (glassy), which influences the kinetics of mass transport, gas uptake, and partitioning (Shiraiwa et al., 2011; Berkemeier et al., 2013; Shiraiwa et al., 2014). Earlier studies have shown that diffusivity-limitations can affect the water uptake, heterogeneous chemical transformation, evaporation, and size distribution of organic aerosol particles (Pfrang et al., 2011; Zhou et al., 2013; Arangio et al., 2015; Berkemeier et al., 2014, 2016; Mu et al., 2018; Zaveri et al., 2020; Berkemeier et al., 2020; Schervish et al., 2026; Kang et al., 2026).

Here, we re-analyze observational data of nanoparticle growth from field measurements in the boreal forest (Hyytiälä, Finland) and from sophisticated laboratory experiments (CERN CLOUD), utilizing a new kinetic multilayer model of multiphase chemistry (KM3C) that resolves the reactivity, diffusivity, and concentration gradients of different chemical species across the gas phase, condensed phase, and the interface between them. We demonstrate that SOA nanoparticle growth can be accurately predicted when the relevant thermodynamic and kinetic aspects of aerosol properties, processes, and temperature dependencies are taken into account in an integrative approach of data analysis and numerical modeling.

## 2 Results and Discussion

Figure 1 illustrates how the elucidation of condensed-phase diffusivity and concentration profiles inside SOA particles resolves previously unexplained discrepancies between field measurements and model predictions of condensable organic vapor concentrations and nanoparticle growth rates. As shown in Fig. 1a and reported by Stolzenburg et al. (2025), nanoparticle growth rates observed in the boreal forest summer (Hyytiälä, Finland, 17 August 2020, blue markers; Gonzalez Carracedo et al., 2022) were substantially lower than those predicted with a traditional kinetic model based on measured concentrations of condensable organic vapors (brown lines and shading). In their modeling approach, Stolzenburg et al. considered uncertainties in the quantification of measured condensable vapors, activity coefficients, and decomposition reactions. They used a two-film model (Zaveri et al., 2014) to investigate the effect of low diffusivity ( $< 10^{-15}$   $\text{cm}^2 \text{s}^{-1}$ ) but could not substantially reduce the gap between observational data and model results (Fig. 1a, brown line and shading; Stolzenburg et al., 2025).

In contrast, our multilayer model KM3C is able to reproduce the observed nanoparticle growth assuming a diffusivity characteristic for highly viscous, nearly glassy semi-solid substances ( $10^{-20}$   $\text{cm}^2 \text{s}^{-1}$ ) and otherwise identical model parameters such as the time-dependent concentrations of condensable organic vapors, their enthalpies of vaporization, and the treatment of the Kelvin effect (Supplementary Information, Sect. S1). As illustrated in Fig. 1c, the low diffusivity leads to the development of differential concentration gradients inside the nanoparticle, where the outer layers contain higher fractions of relatively more volatile compounds (low-volatile organic compounds, LVOC) compared to the inner layers, which in turn show higher fractions of relatively less volatile compounds (ultra low-volatile organic compounds, ULVOC). In other words, the low diffusivity leads to an enrichment of relatively more volatile compounds at the surface, decelerates their uptake into the particle bulk



(surface-to-bulk transport), and delays the equilibration of gas-particle partitioning. These effects keep the particle growth rate lower than expected under the assumption of a well-mixed and thus rapidly equilibrating particle phase (Fig. S1).

Another nanoparticle growth event observed in the boreal forest spring (Hyytiälä, Finland, 11 April 2020) was well captured  
60 by both the two-film model of Stolzenburg et al. (2025) as well as our multilayer model with higher diffusivity ( $10^{-15} \text{ cm}^2 \text{ s}^{-1}$ ; Fig. 1b). Under these conditions, the multilayer model shows a well mixed bulk without differential concentration gradients (Fig. 1d), which does not lead to diffusivity-related limitations of the observed and simulated nanoparticle growth rates.

Assuming different phase states and diffusivities of SOA nanoparticles in the investigated growth events is consistent with earlier studies. These studies showed that SOA particles formed in boreal, mid-latitude, and tropical forests vary between  
65 liquid, semi-solid and glassy phase states depending on aerosol composition, particle size, and ambient conditions such as temperature and humidity (Mikhailov et al., 2009; Virtanen et al., 2010; Koop et al., 2011; Saukko et al., 2012; Renbaum-Wolff et al., 2013; Cheng et al., 2015; Bateman et al., 2016; Slade et al., 2019; Artaxo et al., 2022). While the relative humidity during the two particle growth events displayed in Fig. 1 was essentially the same ( $\sim 50\% \text{ RH}$ ), the ambient temperature was higher in August ( $17.5^\circ\text{C}$ ) than in April ( $3.8^\circ\text{C}$ , Stolzenburg et al., 2025). At elevated temperatures, organic molecules that  
70 partition into the particle phase are expected to be more oxygenated to reach low-enough vapor pressures (Donahue et al., 2011; Shiraiwa et al., 2014; Bilde et al., 2015). Moreover, photochemical aging may proceed faster in summer and has been shown to increase the viscosity of organic aerosols (Antossian et al., 2025; Golay et al., 2026). Due to differences in chemical composition and because the enthalpies of vaporization may exceed activation energies of diffusion (Epstein et al., 2010; Kiland et al., 2019), the diffusivity in organic matter condensing at high temperature may indeed be lower than in organic  
75 matter condensing at low temperature. The volatilities of organic compounds show Arrhenius-behavior following the Clausius-Clapeyron equation, but the viscosity of organic liquids approaching the glass transition generally exhibits super-Arrhenius behavior following the Vogel-Fulcher-Tammann equation (Bilde et al., 2015; Shiraiwa et al., 2017). In semi-solids, activation energies of diffusion may be smaller than enthalpies of vaporization, which would entail a hardening of organic aerosols towards higher temperatures. For glassy organics, however, activation energies of diffusion may be larger than enthalpies of  
80 vaporization and the dependence may reverse: a liquefaction of organic aerosols towards higher temperatures.

Figure 2 shows nanoparticle growth rates measured under very well defined conditions in the CERN CLOUD chamber (Stolzenburg et al., 2018). For particles in the diameter range of 1.5 to 3 nm (Fig. 2a), the growth rates observed at  $5^\circ\text{C}$  are near the kinetic limit derived by Stolzenburg et al. (2025) from the concentration of oxidized organic molecules (OOMs) measured by nitrate chemical ionization mass spectrometry (NO<sub>3</sub>-CIMS). The rates observed at  $-25^\circ\text{C}$  and  $25^\circ\text{C}$ , however, are well above  
85 and below the kinetic limit line, respectively, and were not captured by their modeling approach (Stolzenburg et al., 2025). In the particle size range of 3 to 7 nm (Fig. 2b), the observed growth rates are close to the reported kinetic limit at  $5^\circ\text{C}$  and  $25^\circ\text{C}$ , but again much higher at  $-25^\circ\text{C}$ .

When considering only the OOMs measured by NO<sub>3</sub>-CIMS (Fig. S2), our kinetic multilayer model was also not able to reproduce the observed growth rates. Thus, we included organic vapors measured by proton-transfer reaction time-of-flight  
90 mass spectrometry (PTR3) and integrated the Clausius-Clapeyron equation in KM3C to describe the temperature-dependent volatility distribution of organic vapors (Supplementary Information, Sect. S1). With this approach, we can capture both the

concentration dependence and the temperature dependence of the measured nanoparticle growth rates as illustrated in Figs. 2a,b. Our results show that all available measurement techniques and data (NO<sub>3</sub>-CIMS and PTR3) are needed to cover the full range and variability of condensable organic vapors, including semi-volatile organic compounds (SVOC) that can substantially contribute to nanoparticle growth at -25°C even if their contribution is negligible at +25°C (Fig. S3).

Figure 3 shows a wide range of atmospheric nanoparticle growth rates plotted against organic vapor concentrations as observed in the Asian megacity of Beijing (China, Qiao et al., 2021), at the Europe rural background site San Pietro di Capofiume (Italy, Cai et al., 2024), and at the boreal forest site Hyytiälä (Finland, Gonzalez Carracedo et al., 2022) alongside the CERN CLOUD chamber data as presented by Stolzenburg et al. (2025). Similar to the chamber experiments (circular markers), the field measurement data (diamond markers) exhibit a pronounced increase of OOMs concentrations with increasing temperature (color coding), which can be attributed to general trends of temperature-related enhancements in emissions of volatile organic compounds (VOC) as SOA precursors and photochemical reactivity leading to higher OOMs production rates in the atmosphere (Seinfeld and Pandis, 2016; Paasonen et al., 2018; Bianchi et al., 2019). While the OOMs concentrations vary by three orders of magnitude, the nanoparticle growth rates observed in the atmosphere remain rather uniformly confined to a narrow range around 1 to 10 nm h<sup>-1</sup>.

The field measurement data points and their weak dependence on ambient temperature and OOMs concentration do not follow the dashed black line representing the concentration dependence and kinetic limit of nanoparticle growth as calculated and reported by Stolzenburg et al. (2025). In contrast, the solid black line illustrates the weak OOMs concentration dependence we obtain using KM3C to predict SOA nanoparticle growth rates as a function of temperature and organic vapor concentration assuming the same volatility distributions (volatility basis sets, VBS; Donahue et al., 2006, 2011; Bhattacharyya et al., 2025) as observed in the CERN CLOUD experiments (square markers). As illustrated by the grey shaded areas in Fig. 3, most of the growth rates observed in the field measurements and laboratory experiments reported by Stolzenburg et al. (2025) fall within a factor of three relative to this line.

The tilt and flattening of the high OOMs concentration dependence as obtained by kinetic modeling in earlier studies (Stolzenburg et al., 2018, 2025) towards the low OOMs concentration dependence that we obtained using KM3C in this study can be attributed to the following key factors: (I) at low temperature and OOMs concentration levels, organic vapors that would have relatively high volatility at room temperature can also contribute to nanoparticle growth (upward shift indicated by the arrow on the left side of Figs. 3a,b); and (II) at high temperature and OOMs concentration levels, enhanced volatility, low diffusivity, slow surface-to-bulk transport, and differential concentration gradients decelerate the uptake of organic vapors and delay the equilibration of gas-particle partitioning (downward shift indicated by the arrow on the right side of Figs. 3a,b).

Overall, the variability and temperature dependencies of condensable organic vapor (OOMs) production by VOC oxidation, volatility, and diffusivity are partly offsetting and balancing each other. This balancing leads to an effective buffering of the vapor concentration dependence of atmospheric nanoparticle growth rates around 1 to 10 nm h<sup>-1</sup> as observed and reported in earlier studies (Kulmala et al., 2004; Kulmala and Kerminen, 2008; Stolzenburg et al., 2023, 2025).



### 125 3 Conclusions and Outlook

This study provides an answer to the long-standing and enigmatic scientific question why atmospheric nanoparticle growth rates are fairly uniform under widely different ambient conditions and exhibit a low dependence on organic vapor concentration (OOMs). We have developed and applied a new kinetic multilayer model of multiphase chemistry (KM3C) to explain and reconcile discrepancies between field observations, laboratory experiments, theoretical considerations, and earlier model predictions by resolving the interplay and counteracting effects of temperature-dependent multiphase chemical reactivity, volatility, and diffusivity.

As illustrated in Fig. 4, we identified key factors that lead to an effective buffering and convergence of atmospheric nanoparticle growth rates around 1-10 nm h<sup>-1</sup> in spite of highly variable ambient conditions, including temperature and organic vapor concentrations. The emission and oxidation of organic compounds that serve as SOA precursors, and the production and concentration of potentially condensable organic vapors in the atmosphere generally tend to increase with increasing temperature. At the same time, however, increasing temperature enhances the volatility and equilibrium vapor pressure of organic compounds, thus reducing the proportions of organic compounds that are actually available to condense under equilibrium conditions in accordance with the Clausius-Clapeyron equation (left side of Fig. 4).

Depending on temperature, chemical composition, and size, aerosol particles can adopt a variety of liquid, semi-solid, or solid phase states with widely varying viscosities and diffusivities. The diffusivity can be related to the standard volatility of the organic compounds (saturation mass concentration  $C_{298}^*$ ) that constitute the particles, with larger and more oxidized molecules having lower standard volatility and causing a more viscous phase state of organic aerosols at higher temperatures (Schervish et al., 2026; Kang et al., 2026). Low diffusivity in highly viscous, semi-solid or solid particles can decelerate and kinetically limit the uptake and surface-to-bulk transport of organic vapor molecules, generate differential concentration gradients of compounds with different volatilities in the particle, and delay the equilibration of gas-particle partitioning (right side of Fig. 4). This kinetic limitation can inhibit and effectively buffer particle growth especially at high organic vapor concentration.

The combination and interplay of these effects can explain the previously enigmatic observation of similar growth rates in nanoparticle growth events with vastly different organic vapor concentrations as observed in well-defined laboratory experiments and ambient air around the world. To reproduce the measurement results from the nanoparticle growth events investigated in this study, we did not have to invoke chemical reactions in the condensed phase or at the surface of the particles as suggested in related earlier studies (Heitto et al., 2022; Stolzenburg et al., 2025). Nevertheless, such multiphase chemical reactions - in particular the formation of dimers and oligomers - may also influence the volatility distribution and particle diffusivity, and can be flexibly included in KM3C (Kang et al., 2026).

To further constrain key parameters and enhance the mechanistic understanding and predictability of nanoparticle growth under varying atmospheric conditions, we suggest to perform further laboratory experiments and field observations in which particle phase state and diffusivity are determined alongside condensable vapor concentrations. Especially at low temperatures, extra care should be taken to capture the volatility distribution of all potentially condensable vapors by combining NO<sub>3</sub>-CIMS with PTR3 or other suitable measurement techniques. Kinetic process models, machine learning tools, and targeted uncer-



160 tainty analysis combined in a numerical compass approach can aid the experimental design and help identify the experimental  
conditions that promise the largest gain of mechanistic understanding (Krüger et al., 2024). To achieve a full mechanistic and  
predictive understanding of atmospheric nanoparticle growth, we suggest and intend to further pursue and elaborate the in-  
tegrative approach of data analysis and numerical modeling developed in this study, which has enabled the reconciliation of  
previously unexplained discrepancies between field observations and laboratory experiments, and theoretical considerations.

165 *Code and data availability.* The measurement data were adopted from Stolzenburg et al. (2018) and Stolzenburg et al. (2025). The KM3C  
model code is in preparation for public release as open source code.

*Author contributions.* TB and UP conceived the study. TB designed and supervised research. ZZ, HGK and TB built the kinetic model. ZZ  
performed kinetic model simulations and processed results. All authors analyzed and discussed the results, and co-wrote the paper led by TB  
and UP.

*Competing interests.* At least one of the (co-)authors is a member of the editorial board of ACP.

170 *Acknowledgements.* This work was funded by the Max Planck Society (MPG). HGK is supported by the Max Planck Graduate Center  
with the Johannes Gutenberg University Mainz (MPGC). The authors thank the Max Planck Computing and Data Facility (MPCDF) for  
computing time on the supercomputer RAVEN. We thank A. Mishra, M. Radecka, and colleagues across the scientific community for helpful  
discussions.



## References

- 175 Antossian, C., Müller, M., and Krieger, U. K.: Photochemical and ozone-induced aging significantly alter the viscosity of aqueous *trans*-aconitic acid aerosol particles, *EGUsphere*, 2025, 1–34, <https://doi.org/10.5194/egusphere-2025-5928>, 2025.
- Arangio, A. M., Slade, J. H., Berkemeier, T., Pöschl, U., Knopf, D. A., and Shiraiwa, M.: Multiphase Chemical Kinetics of OH Radical Uptake by Molecular Organic Markers of Biomass Burning Aerosols: Humidity and Temperature Dependence, Surface Reaction, and Bulk Diffusion, *J. Phys. Chem. A*, 119, 4533–4544, <https://doi.org/10.1021/jp510489z>, 2015.
- 180 Artaxo, P., Hansson, H.-C., Andreae, M. O., Bäck, J., Alves, E. G., Barbosa, H. M. J., Bender, F., Bourtsoukidis, E., Carbone, S., Chi, J., Decesari, S., Després, V. R., Ditas, F., Ezhova, E., Fuzzi, S., Hasselquist, N. J., Heintzenberg, J., Holanda, B. A., Guenther, A., Hakola, H., Heikkinen, L., Kerminen, V.-M., Kontkanen, J., Krejci, R., Kulmala, M., Lavric, J. V., de Leeuw, G., Lehtipalo, K., Machado, L. A. T., McFiggans, G., Franco, M. A. M., Meller, B. B., Morais, F. G., Mohr, C., Morgan, W., Nilsson, M. B., Peichl, M., Petäjä, T., Praß, M., Pöhlker, C., Pöhlker, M. L., Pöschl, U., Von Randow, C., Riipinen, I., Rinne, J., Rizzo, L. V., Rosenfeld, D., Silva Dias, M.
- 185 A. F., Sogacheva, L., Stier, P., Swietlicki, E., Sörgel, M., Tunved, P., Virkkula, A., Wang, J., Weber, B., Yáñez-Serrano, A. M., Zieger, P., Mikhailov, E., Smith, J. N., and Kesselmeier, J.: Tropical and Boreal Forest – Atmosphere Interactions: A Review, *Tellus B: Chem. Phys. Meteorol.*, <https://doi.org/10.16993/tellusb.34>, 2022.
- Bateman, A. P., Gong, Z., Liu, P., Sato, B., Cirino, G., Zhang, Y., Artaxo, P., Bertram, A. K., Manzi, A. O., Rizzo, L. V., Souza, R. A. F., Zaveri, R. A., and Martin, S. T.: Sub-micrometre particulate matter is primarily in liquid form over Amazon rainforest, *Nat. Geosci.*, 9, 34–37, <https://doi.org/10.1038/ngeo2599>, 2016.
- 190 Berkemeier, T., Huisman, A. J., Ammann, M., Shiraiwa, M., Koop, T., and Pöschl, U.: Kinetic regimes and limiting cases of gas uptake and heterogeneous reactions in atmospheric aerosols and clouds: a general classification scheme, *Atmos. Chem. Phys.*, 13, 6663–6686, <https://doi.org/10.5194/acp-13-6663-2013>, 2013.
- Berkemeier, T., Shiraiwa, M., Pöschl, U., and Koop, T.: Competition between water uptake and ice nucleation by glassy organic aerosol particles, *Atmos. Chem. Phys.*, 14, 12 513–12 531, <https://doi.org/10.5194/acp-14-12513-2014>, 2014.
- 195 Berkemeier, T., Steimer, S. S., Krieger, U. K., Peter, T., Pöschl, U., Ammann, M., and Shiraiwa, M.: Ozone uptake on glassy, semi-solid and liquid organic matter and the role of reactive oxygen intermediates in atmospheric aerosol chemistry, *Phys. Chem. Chem. Phys.*, 18, 12 662–12 674, <https://doi.org/10.1039/C6CP00634E>, 2016.
- Berkemeier, T., Takeuchi, M., Eris, G., and Ng, N. L.: Kinetic modeling of formation and evaporation of secondary organic aerosol from NO<sub>3</sub> oxidation of pure and mixed monoterpenes, *Atmos. Chem. Phys.*, 20, 15 513–15 535, <https://doi.org/10.5194/acp-20-15513-2020>, 2020.
- 200 Bhattacharyya, N., Lopez, B., DeVivo, J., Russell, D. M., Shen, J., Sommer, E., Almeida, J., Amorim, A., Beckmann, H. M., Busato, M., Canagaratna, M. R., Caudillo, L., Chassaing, A., Christoudias, T., Dada, L., El-Haddad, I., Flagan, R. C., Harder, H., Judmaier, B., Kaniyodical Sebastian, M., Kirkby, J., Klebach, H., Kulmala, M., Kunkler, F., Lehtipalo, K., Liu, L., Mentler, B., Möhler, O., Morawiec, A., Petäjä, T., Rato, P., Rörup, B., Ruhl, S., Scholz, W., Simon, M., Tóme, A., Tong, Y., Top, J., Umo, N. S., Volkamer, R., Weissbacher, J., Worsnop, D. R., Xenofontos, C., Yang, B., Yu, W., Zauner-Wieczorek, M., Zgheib, I., Zhang, J., Zheng, Z., He, X.-C., Stolzenburg, D., Schobesberger, S., Curtius, J., and Donahue, N. M.: Isoprene Aerosol Growth in the Upper Troposphere: Application of the Diagonal Volatility Basis Set to CLOUD Chamber Measurements, *ACS ES&T Air*, 2, 2092–2104, <https://doi.org/10.1021/acsestair.5c00106>, 2025.
- 205 Bianchi, F., Tröstl, J., Junninen, H., Frege, C., Henne, S., Hoyle, C. R., Molteni, U., Herrmann, E., Adamov, A., Bukowiecki, N., Chen, X., Duplissy, J., Gysel, M., Hutterli, M., Kangasluoma, J., Kontkanen, J., Kürten, A., Manninen, H. E., Münch, S., Peräkylä, O., Petäjä, T., Rondo, L., Williamson, C., Weingartner, E., Curtius, J., Worsnop, D. R., Kulmala, M., Dommen, J., and Baltensperger, U.: New particle
- 210



- formation in the free troposphere: A question of chemistry and timing, *Science*, 352, 1109–1112, <https://doi.org/10.1126/science.aad5456>, 2016.
- 215 Bianchi, F., Kurtén, T., Riva, M., Mohr, C., Rissanen, M. P., Roldin, P., Berndt, T., Crounse, J. D., Wennberg, P. O., Mentel, T. F., Wildt, J., Junninen, H., Jokinen, T., Kulmala, M., Worsnop, D. R., Thornton, J. A., Donahue, N., Kjaergaard, H. G., and Ehn, M.: Highly Oxygenated Organic Molecules (HOM) from Gas-Phase Autoxidation Involving Peroxy Radicals: A Key Contributor to Atmospheric Aerosol, *Chem. Rev.*, 119, 3472–3509, <https://doi.org/10.1021/acs.chemrev.8b00395>, 2019.
- 220 Bilde, M., Barsanti, K., Booth, M., Cappa, C. D., Donahue, N. M., Emanuelsson, E. U., McFiggans, G., Krieger, U. K., Marcolli, C., Topping, D., Ziemann, P., Barley, M., Clegg, S., Dennis-Smith, B., Hallquist, M., Hallquist, M., Khlystov, A., Kulmala, M., Mogensen, D., Percival, C. J., Pope, F., Reid, J. P., Ribeiro da Silva, M. A. V., Rosenoern, T., Salo, K., Soonsin, V. P., Yli-Juuti, T., Prisle, N. L., Pagels, J., Rarey, J., Zardini, A. A., and Riipinen, I.: Saturation Vapor Pressures and Transition Enthalpies of Low-Volatility Organic Molecules of Atmospheric Relevance: From Dicarboxylic Acids to Complex Mixtures, *Chem. Rev.*, 115, 4115–4156, <https://doi.org/10.1021/cr5005502>, 2015.
- 225 Cai, J., Sulo, J., Gu, Y., Holm, S., Cai, R., Thomas, S., Neuberger, A., Mattsson, F., Paglione, M., Decesari, S., Rinaldi, M., Yin, R., Aliaga, D., Huang, W., Li, Y., Gramlich, Y., Ciarelli, G., Quéléver, L., Sarnela, N., Lehtipalo, K., Zannoni, N., Wu, C., Nie, W., Kangasluoma, J., Mohr, C., Kulmala, M., Zha, Q., Stolzenburg, D., and Bianchi, F.: Elucidating the mechanisms of atmospheric new particle formation in the highly polluted Po Valley, Italy, *Atmos. Chem. Phys.*, 24, 2423–2441, <https://doi.org/10.5194/acp-24-2423-2024>, 2024.
- Cheng, Y., Su, H., Koop, T., Mikhailov, E., and Pöschl, U.: Size dependence of phase transitions in aerosol nanoparticles, *Nat. Commun.*, 6, 5923, <https://doi.org/10.1038/ncomms6923>, 2015.
- 230 Donahue, N. M., Robinson, A. L., Stanier, C. O., and Pandis, S. N.: Coupled Partitioning, Dilution, and Chemical Aging of Semivolatile Organics, *Environ. Sci. Technol.*, 40, 2635–2643, <https://doi.org/10.1021/es052297c>, 2006.
- Donahue, N. M., Epstein, S. A., Pandis, S. N., and Robinson, A. L.: A two-dimensional volatility basis set: 1. organic-aerosol mixing thermodynamics, *Atmos. Chem. Phys.*, 11, 3303–3318, <https://doi.org/10.5194/acp-11-3303-2011>, 2011.
- Epstein, S. A., Riipinen, I., and Donahue, N. M.: A Semiempirical Correlation between Enthalpy of Vaporization and Saturation Concentration for Organic Aerosol, *Environ. Sci. Technol.*, 44, 743–748, <https://doi.org/10.1021/es902497z>, pMID: 20025284, 2010.
- 235 Golay, Z. M., Vandergrift, G. W., Kamal, S., China, S., Nizkorodov, S. A., and Bertram, A. K.: Sunlight can turn smoldering pine wood smoke into a glass, *npj Clean Air*, 2, 29, <https://doi.org/10.1038/s44407-026-00070-9>, 2026.
- Gonzalez Carracedo, L., Lehtipalo, K., Ahonen, L. R., Sarnela, N., Holm, S., Kangasluoma, J., Kulmala, M., Winkler, P. M., and Stolzenburg, D.: On the relation between apparent ion and total particle growth rates in the boreal forest and related chamber experiments, *Atmos. Chem. Phys.*, 22, 13 153–13 166, <https://doi.org/10.5194/acp-22-13153-2022>, 2022.
- 240 Gordon, H., Kirkby, J., Baltensperger, U., Bianchi, F., Breitenlechner, M., Curtius, J., Dias, A., Dommen, J., Donahue, N. M., Dunne, E. M., Duplissy, J., Ehrhart, S., Flagan, R. C., Frege, C., Fuchs, C., Hansel, A., Hoyle, C. R., Kulmala, M., Kürten, A., Lehtipalo, K., Makhmutov, V., Molteni, U., Rissanen, M. P., Stozkhov, Y., Tröstl, J., Tsagkogeorgas, G., Wagner, R., Williamson, C., Wimmer, D., Winkler, P. M., Yan, C., and Carslaw, K. S.: Causes and importance of new particle formation in the present-day and preindustrial atmospheres, *J. Geophys. Res.: Atmos.*, 122, 8739–8760, <https://doi.org/10.1002/2017jd026844>, 2017.
- 245 Heitto, A., Lehtinen, K., Petäjä, T., Lopez-Hilfiker, F., Thornton, J. A., Kulmala, M., and Yli-Juuti, T.: Effects of oligomerization and decomposition on the nanoparticle growth: a model study, *Atmos. Chem. Phys.*, 22, 155–171, <https://doi.org/10.5194/acp-22-155-2022>, 2022.



- IPCC: Climate Change 2023: Synthesis Report. Contribution of Working Groups I, II and III to the Sixth Assessment Report of the Intergovernmental Panel on Climate Change, <https://doi.org/10.59327/IPCC/AR6-9789291691647>, 2023.
- 250 Jimenez, J. L., Canagaratna, M. R., Donahue, N. M., Prevot, A. S. H., Zhang, Q., Kroll, J. H., DeCarlo, P. F., Allan, J. D., Coe, H., Ng, N. L., Aiken, A. C., Docherty, K. S., Ulbrich, I. M., Grieshop, A. P., Robinson, A. L., Duplissy, J., Smith, J. D., Wilson, K. R., Lanz, V. A., Hueglin, C., Sun, Y. L., Tian, J., Laaksonen, A., Raatikainen, T., Rautiainen, J., Vaattovaara, P., Ehn, M., Kulmala, M., Tomlinson, J. M., Collins, D. R., Cubison, M. J., Dunlea, J., Huffman, J. A., Onasch, T. B., Alfarra, M. R., Williams, P. I., Bower, K., Kondo, Y., Schneider, J., Drewnick, F., Borrmann, S., Weimer, S., Demerjian, K., Salcedo, D., Cottrell, L., Griffin, R., Takami, A., Miyoshi, T., Hatakeyama, S.,
- 255 Shimono, A., Sun, J. Y., Zhang, Y. M., Dzepina, K., Kimmel, J. R., Sueper, D., Jayne, J. T., Herndon, S. C., Trimborn, A. M., Williams, L. R., Wood, E. C., Middlebrook, A. M., Kolb, C. E., Baltensperger, U., and Worsnop, D. R.: Evolution of Organic Aerosols in the Atmosphere, *Science*, 326, 1525–1529, <https://doi.org/10.1126/science.1180353>, 2009.
- Kang, H. G., Takeuchi, M., Ng, N. L., Pöschl, U., and Berkemeier, T.: Multiphase Chemistry and Phase State Explain Nonlinear Effects in the Formation and Evaporation of SOA from Mixed Monoterpene Precursors, *ACS ES&T Air*, <https://doi.org/10.1021/acsestair.5c00438>,
- 260 2026.
- Kiland, K. J., Maclean, A. M., Kamal, S., and Bertram, A. K.: Diffusion of Organic Molecules as a Function of Temperature in a Sucrose Matrix (a Proxy for Secondary Organic Aerosol), *J. Phys. Chem. Lett.*, 10, 5902–5908, <https://doi.org/10.1021/acs.jpcclett.9b02182>, 2019.
- Koop, T., Bookhold, J., Shiraiwa, M., and Pöschl, U.: Glass transition and phase state of organic compounds: dependency on molecular properties and implications for secondary organic aerosols in the atmosphere, *Phys. Chem. Chem. Phys.*, 13, 19238, <https://doi.org/10.1039/c1cp22617g>, 2011.
- 265 Krüger, M., Mishra, A., Spichtinger, P., Pöschl, U., and Berkemeier, T.: A numerical compass for experiment design in chemical kinetics and molecular property estimation, *J. Cheminf.*, 16, 34, <https://doi.org/10.1186/s13321-024-00825-0>, 2024.
- Kulmala, M. and Kerminen, V.-M.: On the formation and growth of atmospheric nanoparticles, *Atmos. Res.*, 90, 132–150, <https://doi.org/https://doi.org/10.1016/j.atmosres.2008.01.005>, 2008.
- 270 Kulmala, M., Vehkamäki, H., Petäjä, T., Dal Maso, M., Lauri, A., Kerminen, V.-M., Birmili, W., and McMurry, P.: Formation and growth rates of ultrafine atmospheric particles: a review of observations, *J. Aerosol Sci.*, 35, 143–176, <https://doi.org/10.1016/j.jaerosci.2003.10.003>, 2004.
- Kulmala, M., Petäjä, T., Ehn, M., Thornton, J., Sipilä, M., Worsnop, D., and Kerminen, V.-M.: Chemistry of Atmospheric Nucleation: On the Recent Advances on Precursor Characterization and Atmospheric Cluster Composition in Connection with Atmospheric New Particle
- 275 Formation, *Annu. Rev. Phys. Chem.*, 65, 21–37, <https://doi.org/10.1146/annurev-physchem-040412-110014>, 2014.
- Kulmala, M., Cai, R., Stolzenburg, D., Zhou, Y., Dada, L., Guo, Y., Yan, C., Petäjä, T., Jiang, J., and Kerminen, V.-M.: The contribution of new particle formation and subsequent growth to haze formation, *Environ. Sci.: Atmos.*, 2, 352–361, <https://doi.org/10.1039/D1EA00096A>, 2022.
- Mikhailov, E., Vlasenko, S., Martin, S. T., Koop, T., and Pöschl, U.: Amorphous and crystalline aerosol particles interacting with water vapor: conceptual framework and experimental evidence for restructuring, phase transitions and kinetic limitations, *Atmos. Chem. Phys.*, 9, 9491–9522, <https://doi.org/10.5194/acp-9-9491-2009>, 2009.
- 280 Mu, Q., Shiraiwa, M., Octaviani, M., Ma, N., Ding, A., Su, H., Lammel, G., Pöschl, U., and Cheng, Y.: Temperature effect on phase state and reactivity controls atmospheric multiphase chemistry and transport of PAHs, *Sci. Adv.*, 4, eaap7314, <https://doi.org/10.1126/sciadv.aap7314>, 2018.



- 285 Paasonen, P., Peltola, M., Kontkanen, J., Junninen, H., Kerminen, V.-M., and Kulmala, M.: Comprehensive analysis of particle growth rates from nucleation mode to cloud condensation nuclei in boreal forest, *Atmos. Chem. Phys.*, 18, 12 085–12 103, <https://doi.org/10.5194/acp-18-12085-2018>, 2018.
- Pfrang, C., Shiraiwa, M., and Pöschl, U.: Chemical ageing and transformation of diffusivity in semi-solid multi-component organic aerosol particles, *Atmos. Chem. Phys.*, 11, 7343–7354, <https://doi.org/10.5194/acp-11-7343-2011>, 2011.
- 290 Qiao, X., Yan, C., Li, X., Guo, Y., Yin, R., Deng, C., Li, C., Nie, W., Wang, M., Cai, R., Huang, D., Wang, Z., Yao, L., Worsnop, D. R., Bianchi, F., Liu, Y., Donahue, N. M., Kulmala, M., and Jiang, J.: Contribution of Atmospheric Oxygenated Organic Compounds to Particle Growth in an Urban Environment, *Environ. Sci. Technol.*, 55, 13 646–13 656, <https://doi.org/10.1021/acs.est.1c02095>, 2021.
- Reid, J. P., Bertram, A. K., Topping, D. O., Laskin, A., Martin, S. T., Petters, M. D., Pope, F. D., and Rovelli, G.: The viscosity of atmospherically relevant organic particles, *Nat. Commun.*, 9, 956, <https://doi.org/10.1038/s41467-018-03027-z>, 2018.
- 295 Renbaum-Wolff, L., Grayson, J. W., Bateman, A. P., Kuwata, M., Sellier, M., Murray, B. J., Shilling, J. E., Martin, S. T., and Bertram, A. K.: Viscosity of  $\alpha$ -pinene secondary organic material and implications for particle growth and reactivity, *P. Natl. Acad. Sci. USA*, 110, 8014–8019, <https://doi.org/10.1073/pnas.1219548110>, 2013.
- Riipinen, I., Pierce, J. R., Yli-Juuti, T., Nieminen, T., Häkkinen, S., Ehn, M., Junninen, H., Lehtipalo, K., Petäjä, T., Slowik, J., Chang, R., Shantz, N. C., Abbatt, J., Leaitch, W. R., Kerminen, V.-M., Worsnop, D. R., Pandis, S. N., Donahue, N. M., and Kulmala, M.: Organic condensation: a vital link connecting aerosol formation to cloud condensation nuclei (CCN) concentrations, *Atmos. Chem. Phys.*, 11, 3865–3878, <https://doi.org/10.5194/acp-11-3865-2011>, 2011.
- 300 Saukko, E., Lambe, A. T., Massoli, P., Koop, T., Wright, J. P., Croasdale, D. R., Pedernera, D. A., Onasch, T. B., Laaksonen, A., Davidovits, P., Worsnop, D. R., and Virtanen, A.: Humidity-dependent phase state of SOA particles from biogenic and anthropogenic precursors, *Atmos. Chem. Phys.*, 12, 7517–7529, <https://doi.org/10.5194/acp-12-7517-2012>, 2012.
- 305 Schervish, M., Kang, H. G., Wingen, L. M., Nguyen, K., Begay, C., Wilson, J., Shrivastava, M., Chen, Y., Shilling, J. E., Ng, N. L., Pöschl, U., Berkemeier, T., Zelenyuk, A., and Shiraiwa, M.: Surface Crust Formation Controls Evaporation Kinetics of Secondary Organic Aerosols, *Environ. Sci. Technol.*, 60, 7995–8006, <https://doi.org/10.1021/acs.est.5c11018>, 2026.
- Seinfeld, J. H. and Pandis, S. N.: *Atmospheric chemistry and physics: from air pollution to climate change*, John Wiley & Sons, 2016.
- Shiraiwa, M., Ammann, M., Koop, T., and Pöschl, U.: Gas uptake and chemical aging of semisolid organic aerosol particles, *P. Natl. Acad. Sci. USA*, 108, 11 003–11 008, <https://doi.org/10.1073/pnas.1103045108>, 2011.
- 310 Shiraiwa, M., Berkemeier, T., Schilling-Fahnestock, K. A., Seinfeld, J. H., and Pöschl, U.: Molecular corridors and kinetic regimes in the multiphase chemical evolution of secondary organic aerosol, *Atmos. Chem. Phys.*, 14, 8323–8341, <https://doi.org/10.5194/acp-14-8323-2014>, 2014.
- Shiraiwa, M., Li, Y., Tsimpidi, A. P., Karydis, V. A., Berkemeier, T., Pandis, S. N., Lelieveld, J., Koop, T., and Pöschl, U.: Global distribution of particle phase state in atmospheric secondary organic aerosols, *Nat. Commun.*, 8, 15 002, <https://doi.org/10.1038/ncomms15002>, 2017.
- 315 Shrivastava, M., Cappa, C. D., Fan, J., Goldstein, A. H., Guenther, A. B., Jimenez, J. L., Kuang, C., Laskin, A., Martin, S. T., Ng, N. L., Petaja, T., Pierce, J. R., Rasch, P. J., Roldin, P., Seinfeld, J. H., Shilling, J., Smith, J. N., Thornton, J. A., Volkamer, R., Wang, J., Worsnop, D. R., Zaveri, R. A., Zelenyuk, A., and Zhang, Q.: Recent advances in understanding secondary organic aerosol: Implications for global climate forcing, *Rev. Geophys.*, 55, 509–559, <https://doi.org/10.1002/2016RG000540>, 2017.
- 320 Slade, J. H., Ault, A. P., Bui, A. T., Ditto, J. C., Lei, Z., Bondy, A. L., Olson, N. E., Cook, R. D., Desrochers, S. J., Harvey, R. M., Erickson, M. H., Wallace, H. W., Alvarez, S. L., Flynn, J. H., Boor, B. E., Petrucci, G. A., Gentner, D. R., Griffin, R. J., and Shepson, P. B.: Bouncer



- Particles at Night: Biogenic Secondary Organic Aerosol Chemistry and Sulfate Drive Diel Variations in the Aerosol Phase in a Mixed Forest, *Environ. Sci. Technol.*, 53, 4977–4987, <https://doi.org/10.1021/acs.est.8b07319>, PMID: 31002496, 2019.
- 325 Stolzenburg, D., Fischer, L., Vogel, A. L., Heinritzi, M., Schervish, M., Simon, M., Wagner, A. C., Dada, L., Ahonen, L. R., Amorim, A., Baccarini, A., Bauer, P. S., Baumgartner, B., Bergen, A., Bianchi, F., Breitenlechner, M., Brilke, S., Buenrostro Mazon, S., Chen, D., Dias, A., Draper, D. C., Duplissy, J., El Haddad, I., Finkenzeller, H., Frege, C., Fuchs, C., Garmash, O., Gordon, H., He, X., Helm, J., Hofbauer, V., Hoyle, C. R., Kim, C., Kirkby, J., Kontkanen, J., Kürten, A., Lampilahti, J., Lawler, M., Lehtipalo, K., Leiminger, M., Mai, H., Mathot, S., Mentler, B., Molteni, U., Nie, W., Nieminen, T., Nowak, J. B., Ojdanic, A., Onnela, A., Passananti, M., Petäjä, T., Quéléver, L. L. J., Rissanen, M. P., Sarnela, N., Schallhart, S., Tauber, C., Tomé, A., Wagner, R., Wang, M., Weitz, L., Wimmer, D., Xiao, M., Yan, C., Ye, P., Zha, Q., Baltensperger, U., Curtius, J., Dommen, J., Flagan, R. C., Kulmala, M., Smith, J. N., Worsnop, D. R., Hansel, A., Donahue, N. M., and Winkler, P. M.: Rapid growth of organic aerosol nanoparticles over a wide tropospheric temperature range, *P. Natl. Acad. Sci. USA*, 115, 9122–9127, <https://doi.org/10.1073/pnas.1807604115>, 2018.
- 330 Stolzenburg, D., Cai, R., Blichner, S. M., Kontkanen, J., Zhou, P., Makkonen, R., Kerminen, V.-M., Kulmala, M., Riipinen, I., and Kangasluoma, J.: Atmospheric nanoparticle growth, *Rev. Mod. Phys.*, 95, 045 002, <https://doi.org/10.1103/RevModPhys.95.045002>, 2023.
- 335 Stolzenburg, D., Sarnela, N., Bianchi, F., Cai, J., Cai, R., Cheng, Y., Dada, L., Donahue, N. M., Grothe, H., Holm, S., Kerminen, V.-M., Lehtipalo, K., Petäjä, T., Sulo, J., Winkler, P. M., Yan, C., Kangasluoma, J., and Kulmala, M.: Incomplete mass closure in atmospheric nanoparticle growth, *npj Clim. Atmos. Sci.*, 8, <https://doi.org/10.1038/s41612-025-00893-5>, 2025.
- Virtanen, A., Joutsensaari, J., Koop, T., Kannosto, J., Yli-Pirilä, P., Leskinen, J., Mäkelä, J. M., Holopainen, J. K., Pöschl, U., Kulmala, M., Worsnop, D. R., and Laaksonen, A.: An amorphous solid state of biogenic secondary organic aerosol particles, *Nature*, 467, 824–827, <https://doi.org/10.1038/nature09455>, 2010.
- 340 WHO: Health workforce support and safeguards list 2023, Tech. rep., World Health Organization, Geneva, Switzerland, <https://www.who.int/publications/i/item/9789240069787>, accessed: 2026 April 1, 2023.
- Yli-Juuti, T., Mohr, C., and Riipinen, I.: Open questions on atmospheric nanoparticle growth, *Commun. Chem.*, 3, 106, <https://doi.org/10.1038/s42004-020-00339-4>, 2020.
- 345 Zaveri, R. A., Easter, R. C., Shilling, J. E., and Seinfeld, J. H.: Modeling kinetic partitioning of secondary organic aerosol and size distribution dynamics: representing effects of volatility, phase state, and particle-phase reaction, *Atmos. Chem. Phys.*, 14, 5153–5181, <https://doi.org/10.5194/acp-14-5153-2014>, 2014.
- Zaveri, R. A., Shilling, J. E., Zelenyuk, A., Zawadowicz, M. A., Suski, K., China, S., Bell, D. M., Veghte, D., and Laskin, A.: Particle-Phase Diffusion Modulates Partitioning of Semivolatile Organic Compounds to Aged Secondary Organic Aerosol, *Environ. Sci. Technol.*, 54, 2595–2605, <https://doi.org/10.1021/acs.est.9b05514>, 2020.
- 350 Zhou, S., Shiraiwa, M., McWhinney, R. D., Pöschl, U., and Abbatt, J. P. D.: Kinetic limitations in gas-particle reactions arising from slow diffusion in secondary organic aerosol, *Faraday Discuss.*, 165, 391–406, <https://doi.org/10.1039/C3FD00030C>, 2013.
- Zobrist, B., Marcolli, C., Pedernera, D. A., and Koop, T.: Do atmospheric aerosols form glasses?, *Atmos. Chem. Phys.*, 8, 5221–5244, <https://doi.org/10.5194/acp-8-5221-2008>, 2008.

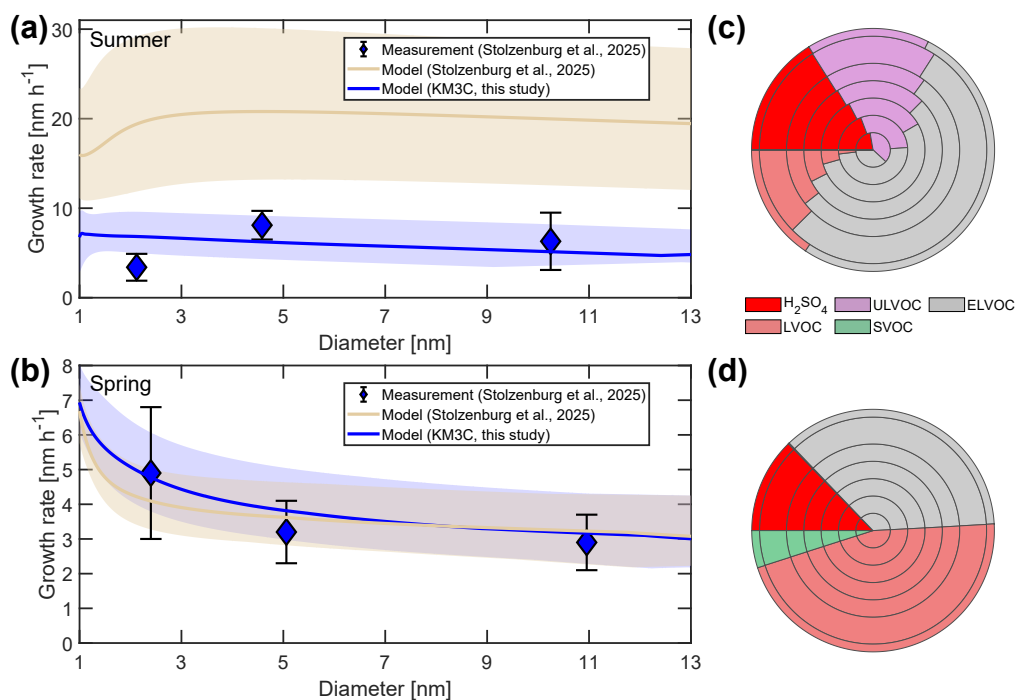


**Figure 1.** Atmospheric nanoparticle growth observed in field measurements. Blue diamond markers and error bars represent arithmetic mean values and standard deviations of growth rates measured in (a) summer and (b) spring at a boreal forest site (Hyytiälä, Finland; Gonzalez Carracedo et al. (2022)). Lines and shadings represent model predictions and uncertainty ranges obtained with a traditional two-film model in brown color (Stolzenburg et al., 2025) and with the new multilayer model KM3C in blue color (Sect. S4). KM3C captures the observations assuming low diffusivity ( $10^{-20}$  cm<sup>2</sup> s<sup>-1</sup>) in summer (a) and high diffusivity ( $10^{-15}$  cm<sup>2</sup> s<sup>-1</sup>) in spring (b). In contrast, the two-film model of (Stolzenburg et al., 2025) reproduced the observations only in spring but not in summer. Radial concentration profiles of sulfuric acid (H<sub>2</sub>SO<sub>4</sub>) and organic compounds with different volatilities (ULVOC, ELVOC, LVOC, SVOC) calculated by KM3C show that the growing particles (7 nm) are well-mixed and contain larger proportions of more volatile compounds (LVOC/SVOC) in spring (d). In summer (c), however, the growing particles contain larger proportions of less volatile compounds (ULVOC/ELVOC) and exhibit differential concentration gradients, which reflect kinetic limitations of mass transport that were not captured by the two-film model.

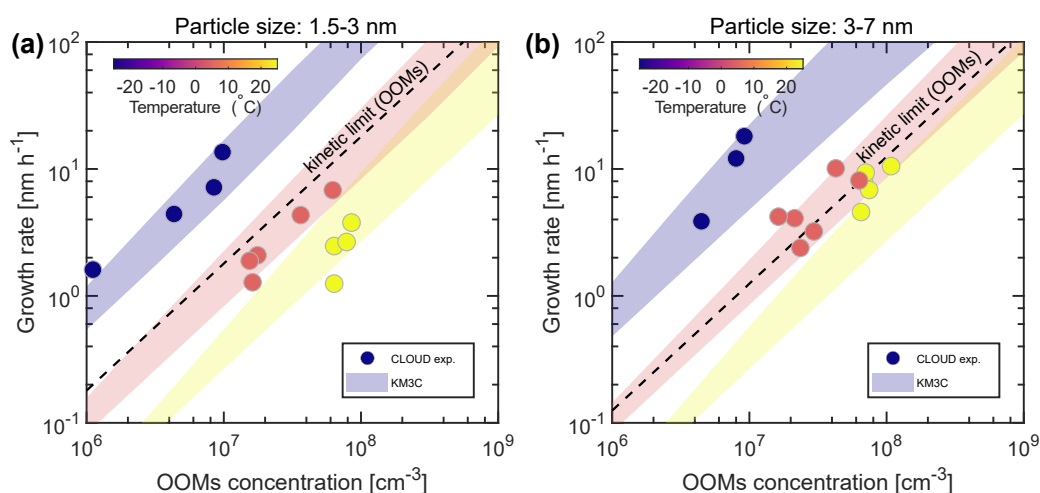


**Figure 2.** Secondary organic aerosol nanoparticle growth observed in laboratory experiments. Circular markers represent growth rates measured at different temperatures in the CERN CLOUD chamber (Stolzenburg et al., 2018, 2025) for particle size ranges of 1.5-3 nm (a) and 3-7 nm (b). The dependence on temperature and concentration of oxygenated organic molecules (OOMs) determined by chemical ionization mass spectrometry (CIMS) was not captured by the modeling approach of Stolzenburg et al. (2025) (dashed line, "kinetic limit (OOMs)"). Considering also more volatile organic compounds detected by proton-transfer reaction time-of-flight mass spectrometry (PTR3, Stolzenburg et al. (2025)) and volatility shifts according to the Clausius-Clapeyron equation, we were able to predict both the temperature and concentration dependence utilizing KM3C (colored bands). The width of the colored bands corresponds to the same range of diffusivities as assumed in Fig. 1 ( $10^{-20}$  -  $10^{-15}$   $\text{cm}^2 \text{s}^{-1}$ ) and detailed in the Supplementary Information (Sect. S5).

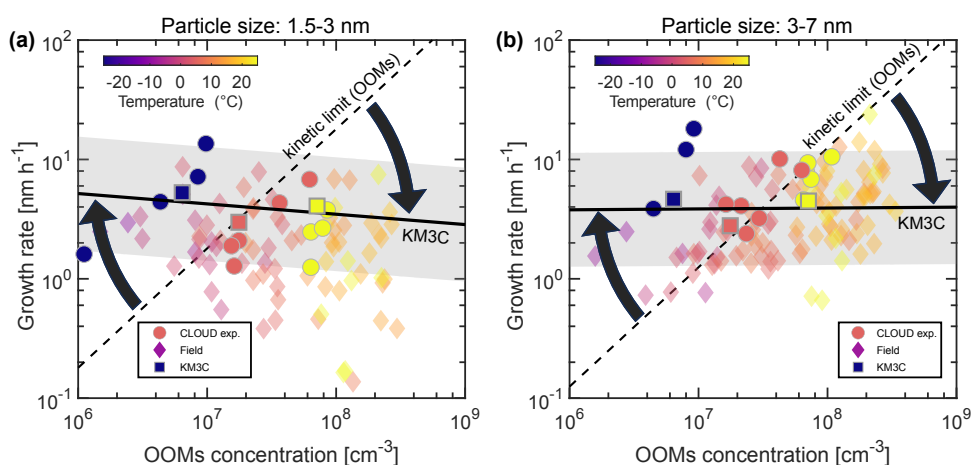


**Figure 3.** Range and buffering of observed and predicted atmospheric nanoparticle growth rates. Measurement data points color-coded by temperature represent growth rates as presented and discussed by Stolzenburg et al. (2025) for particles with diameters in the ranges of (a) 1.5-3 nm and (b) 3-7 nm, respectively. The data are plotted against the concentration of oxygenated organic molecules (OOMs) measured by NO<sub>3</sub>-CIMS during laboratory experiments in the CERN CLOUD chamber (circles, Stolzenburg et al., 2018) and during field measurements (diamonds) in Hyytiälä, Finland (Gonzalez Carracedo et al., 2022), Beijing, China (Qiao et al., 2021), and San Pietro di Capofiume, Italy (Cai et al., 2024). Square markers represent growth rates predicted by KM3C at the temperatures, median organic vapor concentrations and volatility distributions reported for the CERN CLOUD chamber experiments, and the solid black lines are linear fits to the model results. As indicated by the grey shaded areas, most of the growth rates observed in the field measurements and laboratory experiments fall within a factor of three relative to this line. The dashed black line is the kinetic limit reported by Stolzenburg et al. (2025), and the black arrows indicate the effective buffering of the organic vapor (OOMs) concentration dependence of atmospheric nanoparticle growth by temperature-related shifts in diffusivity and volatility.

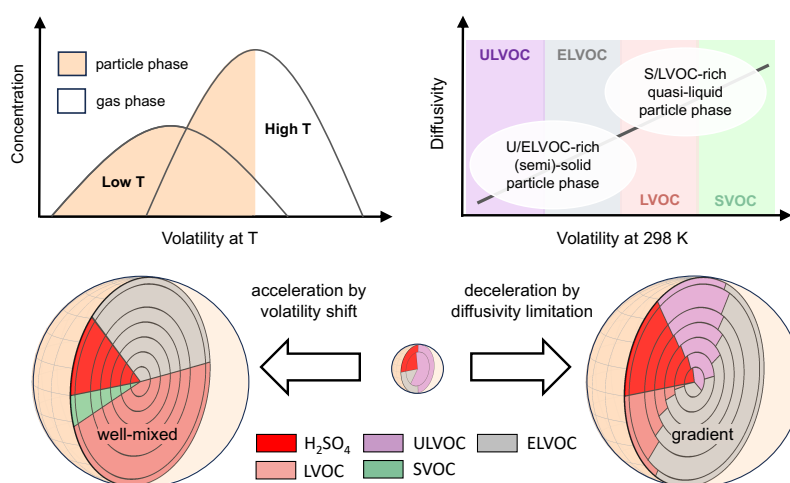


**Figure 4.** Key factors in the buffering of atmospheric nanoparticle growth rates. Ambient temperature influences the production and volatility distribution of condensable vapors in the atmosphere. An increase in temperature tends to enhance the production and concentration of organic vapors, but it also enhances their volatility (equilibrium vapor pressure) following the Clausius-Clapeyron equation and shifts the gas-particle partitioning towards the gas phase. These competing effects buffer the amount of vapors that are available to condense and drive particle growth. In addition, particle composition and phase state are influencing the diffusivity, which tends to increase with increasing volatility of the condensed organic compounds. At elevated temperatures, primarily very low volatile compounds (ULVOC, ELVOC) tend to condense and form (semi)-solid phases with kinetic limitations of diffusivity and surface-to-bulk transport, leading to differential concentration gradients and surface enrichment of more volatile compounds. At low temperatures, also more volatile compounds (SVOC, LVOC) tend to condense and favor the formation of quasi-liquid phases and well-mixed particles that are not subject to kinetic limitations by slow diffusion.